

Characterization of a new Baeyer-Villiger monooxygenase and conversion to a solely N- or S-oxidizing enzyme by a single R292 mutation



Gianluca Catucci^{a,1}, Ivan Zgrablic^{a,1}, Francesco Lanciani^a, Francesca Valetti^a, Daniela Minerdi^a, David P. Ballou^b, Gianfranco Gilardi^a, Sheila J. Sadeghi^{a,*}

^a Department of Life Sciences and Systems Biology, University of Torino, 10123 Turin, Italy

^b Department of Biological Chemistry, University of Michigan, Ann Arbor, MI 48109-0600, USA

ARTICLE INFO

Article history:

Received 16 May 2016

Received in revised form 27 May 2016

Accepted 20 June 2016

Available online 23 June 2016

Keywords:

BVMO

Flavoprotein

Drug metabolites

Stopped-flow

Ethionamide

Isothermal calorimetry

ABSTRACT

Background: Ar-BVMO is a recently discovered Baeyer-Villiger monooxygenase from the genome of *Acinetobacter radioresistens* S13 closely related to medically relevant ethionamide monooxygenase EtaA (prodrug activator) and capable of inactivating the imipenem antibiotic.

Methods: The co-substrate preference as well as steady-state and rapid kinetics studies of the recombinant purified protein were carried out using stopped-flow spectroscopy under anaerobic and aerobic conditions. K_d values were measured by isothermal calorimetry. Enzymatic activity was determined by measuring the amount of product formed using high pressure liquid chromatography or gas chromatography. Site-directed mutagenesis experiments were performed to decipher the role of the active site arginine-292.

Results: Ar-BVMO was found to oxidize ethionamide as well as linear ketones. Mechanistic studies on the wild type enzyme using stopped-flow spectroscopy allowed for the detection of the characteristic oxygenating C4a-(hydro)peroxyflavin intermediate, which decayed rapidly in the presence of the substrate. Replacement of arginine 292 in Ar-BVMO by glycine or alanine resulted in greatly reduced or no Baeyer-Villiger activity, respectively, demonstrating the crucial role of this residue in catalysis of ketone substrates. However, both the R292A and R292G mutants are capable of carrying out N- and S-oxidation reactions.

Conclusions: Substrate profiling of Ar-BVMO confirms its close relationship to EtaA; ethionamide is one of its substrates. The active site Arginine 292 is required for its Baeyer-Villiger activity but not for heteroatom oxidation. **General significance:** A single mutation converts Ar-BVMO to a unique S- or N-monooxygenase, a useful biocatalyst for the production of oxidized metabolites of human drug metabolizing enzymes.

© 2016 Elsevier B.V. All rights reserved.

1. Introduction

Baeyer-Villiger monooxygenases (BVMOs) are flavin-containing enzymes that mediate specific Baeyer-Villiger oxidations on the carbonyl moiety of their substrates. These proteins have great value in the conversion of ketones into corresponding esters and lactones, with wide applications in bioremediation and sustainable biocatalysis. In addition to Baeyer-Villiger oxidations, BVMO enzymes can also catalyze heteroatom oxidations (nitrogen and sulfur) [1] that can have interesting applications to the pharmaceutical industry, as shown by our recent results on the oxidation of the antibiotic imipenem [2].

All BVMO enzymes contain a flavin prosthetic group crucial for their activity, and they use either NADH or NADPH as the electron donor. BVMOs are abundant in bacteria, fungi, and plants but their numbers are limited or zero in animal or human genomes, although it has recently been discovered that some human flavin-containing monooxygenases, such as FMO5, are capable of catalyzing a Baeyer-Villiger oxidation reaction [3].

All BVMO enzymes characterized to date are able to incorporate one atom from molecular oxygen into the substrate while converting the other oxygen into water [4]. The catalytic mechanisms are similar to those previously described in the literature for other flavin-containing oxygenases. In the first step of the catalytic cycle, the cofactor undergoes a 2-electron reduction supposedly via hydride ion transfer from NAD(P)H. The reduced flavin reacts rapidly with molecular oxygen to form a peroxyflavin that is stabilized by the bound NAD(P). After a suitable substrate enters the active site of the enzyme, the flavin peroxide attacks the electrophilic carbonyl of the substrate, resulting in one

* Corresponding author at: Department of Life Sciences and Systems Biology, University of Torino, Via Accademia Albertina 13, 10123 Turin, Italy.

E-mail address: sheila.sadeghi@unito.it (S.J. Sadeghi).

¹ These authors have contributed equally to this work.

atom of molecular oxygen being transferred to the substrate with the other forming water. The formation of the reactive peroxyflavin is independent of substrate binding, distinguishing BVMO enzymes from other flavin-containing hydroxylases and cytochromes P450. In the reaction, the nucleophilic attack of the flavin peroxide on the carbonyl group of the substrate forms a tetrahedral species that is known as a Criegee intermediate, and this rearranges to form an ester that is stereochemically imposed by the enzyme. The product then leaves the active site followed by the release of the NAD(P)⁺ and the cycle can start over again [4–6].

The first BVMO to be studied in detail was cyclohexanone monooxygenases (CHMO) from *Acinetobacter* sp. (NCIMB 9871) [7,8]. Although the genus *Acinetobacter* has been shown to be a source of several BVMO proteins, many of these enzymes are not available in recombinant form and therefore have not yet been characterized. Using sequence homologies and the presence of the conserved Baeyer-Villiger sequence motif, we have recently discovered a novel BVMO, Ar-BVMO, in the genome of *Acinetobacter radioresistens* S13 [9]. This protein was found to share a 49.7% sequence identity and 71.0% sequence similarity with the ethionamide-activating (EtaA) BVMO from *Mycobacterium tuberculosis* [10–12]. Furthermore, phylogenetic analysis of the Ar-BVMO not only placed this protein in the same branch as EtaA but also showed it to be closely related to the phase-1 drug metabolizing enzyme, human flavin-containing monooxygenase 3 (FMO3), but only distantly related to other canonical bacterial BVMO proteins [9,13]. Considering these relationships, initially we studied Ar-BVMO for its possible activities with “unusual/non-typical” substrates and demonstrated that it is not only capable of oxidizing two anticancer drugs metabolized by human FMO3, Danusertib and Tozasertib [14,15], but it can also oxidize other synthetic drugs such as imipenem [2]. Imipenem is a carbapenem, which is a clinically important antibiotic family used in the treatment of MultiDrug-Resistant (MDR) bacterial infections. Interestingly, an identical gene to that of Ar-BVMO also exists in *Acinetobacter Baumannii*, one of the so-called superbugs [2]. In these cases, Ar-BVMO seems to be responsible for the de-activation of this antibiotic, and therefore it acts more like a drug metabolizing enzyme. Chen and coworkers [16] have also shown that a FMO from *Methylocella silvestris* is able to oxidize trimethylamine, which is also a typical substrate of eukaryotic FMO enzymes. The reason(s) why prokaryotic flavin monooxygenases should metabolize substrates that are typically metabolized by the eukaryotic FMO enzymes but not present in prokaryotic natural habitats is still not clear.

In order to better understand these observations, we have undertaken the characterization of the wild type and mutant recombinant Ar-BVMOs. Kinetic studies of Ar-BVMO, as well as investigations into the roles of its active site amino acids thought to be important for BV reactions were carried out. Comparisons of these properties with those of canonical BVMO enzymes were used to try to understand how Ar-BVMO is competent to carry out oxygenations with synthetic and medically relevant drugs.

The role of the active site arginine 292 was also investigated in relation to the enzyme activity towards linear ketones. Two mutants R292A and R292G have no BV activity while still maintaining their S- and N-oxygenation capabilities. These monooxygenation activities are important for human drug metabolism, and therefore, these Ar-BVMO mutants could be useful as bacterial biocatalysts for large-scale production of human drug metabolites.

2. Materials and methods

2.1. Reagents

Riboflavin, NADPH, NADH, ethionamide, 4-phenyl-2-butanone, phenethyl acetate, 2-octanone, hexyl acetate, 2-decanone, octyl acetate, 2-decanone, methyl undecanoate, decyl acetate, acetonitrile,

ethyl acetate, methanol, n-hexane, and salts were purchased from Sigma–Aldrich (Italy).

2.2. Cloning of Ar-BVMO gene in pT7 expression vector

A. radioresistens S13 was isolated from soil surrounding an activated sludge pilot plant (Torino, Italy) and its Ar-BVMO gene was previously isolated by our group from *A. radioresistens* S13 genome by PCR using two primers designed on the basis of the *almA* gene of this species [13]. The product of this PCR was used as the template for the insertion of the desired restriction sites upstream and downstream of the gene for cloning into pT7-7 [17,18].

The BVMO gene was amplified with a nested PCR using primers specifically designed on the basis of the Ar-BVMO coding gene, adding a 6 histidine tag at the C-terminus for ease of purification. The sequences of the primers used were: 5'-AACCAACCAAGGATCCATGGATAAACAC ATTGATGTTCTAATT-3' and 5'-TTGGTTGGTTGAATTCTTAATGGTGATG GTGATGGTGTGAAACCAGTTTAGGTTTACGTTC-3'. The PCR conditions were as follows: denaturation at 94 °C for 3 min; 30 cycles at 94 °C for 30 s, 64 °C for 30 s, and 72 °C for 1 1/2 min; and a final extension at 72 °C for 10 min. A PCR product of the expected size (1541 bp) was obtained. The PCR product was digested with *EcoRI* and *BamHI* restriction enzymes. The linearized insert and pT7-7 vector [17,18], with compatible sticky ends, were used in a ligation reaction to produce the desired clone. *Escherichia coli* BL21 (DE3) competent cells were then transformed with the ligation mixtures and plated on LB agar with 100 µg/mL ampicillin. Colonies with the insert were screened and subsequently the entire pT7-BVMO sequenced.

2.3. Expression of wild-type Ar-BVMO

The expression of the Ar-BVMO enzyme was carried out in a 5 L Biostat A plus fermenter. Forty milliliters of overnight liquid culture of *E. coli* BL21 (DE3) cells transformed with pT7-BVMO were used to inoculate 4 L LB medium supplemented with ampicillin (100 µg/mL) and riboflavin (20 mg/L). The cells were grown at 37 °C and 200 rpm until OD₆₀₀ of 0.5 was reached. At this point, protein expression was induced by the addition of IPTG and the temperature was lowered to 24 °C. The cells were harvested 20 h post-induction by 20 min centrifugation at 4000 rpm at 4 °C.

2.4. Purification of wild-type Ar-BVMO

All purification procedures were carried out at 4 °C. The pellet was resuspended in 50 mL of Buffer A (50 mM KPi pH 7.4, 20% glycerol, 5 mM β-mercaptoethanol) supplemented with 0.5 mM of the protease inhibitor phenylmethylsulfonyl fluoride (PMSF) and 1 mg/mL of lysozyme. The resuspended cells were disrupted by sonication. The lysate was supplemented with 1% Igepal (octylphenoxy polyethoxyethanol), stirred for 30 min at 4 °C to obtain complete homogeneity, and then centrifuged at 4000 rpm for 45 min. The clarified lysate was loaded onto a DEAE-Sepharose Fast-Flow column pre-equilibrated with buffer A. The bound BVMO protein was extensively washed with the same buffer before it was eluted by applying a gradient of 0–250 mM NaCl also in buffer A. Fractions containing the flavoprotein were then pooled and loaded on a Nickel chelating Sepharose Fast-Flow column pre-equilibrated with Buffer B (Buffer A supplemented with 250 mM NaCl). The bound protein was washed with 5 column volumes of Buffer B, 5 column volumes of Buffer B supplemented with 1 mM histidine and 2 column volumes of Buffer B supplemented with 5 mM of histidine. The protein was finally eluted with Buffer B supplemented with 40 mM histidine. Fractions presenting the characteristic FAD peaks were pooled and buffer exchanged with Amicon centrifugal units (30 kDa cut off) with 100 mM potassium phosphate buffer pH 7.4, 20% glycerol.

2.5. Determination of the extinction coefficient of Ar-BVMO

Ar-BVMO was purified as a bright yellow protein containing the flavin cofactor. Spectral analysis of the purified recombinant protein displayed the characteristic flavin spectrum with absorbance maxima at around 375 and 450 nm. The absorbance ratio 280:450 nm of the purified protein was around 10.

Following the method described by Sheng et al. [8], the purified Ar-BVMO was denatured in the presence of 0.1% SDS and the concentration of free FAD released from the enzyme was determined from its extinction coefficient of $11,300 \text{ M}^{-1} \text{ cm}^{-1}$ at 450 nm [19]. Using this procedure the extinction coefficient of Ar-BVMO was determined to be $13,900 \text{ M}^{-1} \text{ cm}^{-1}$ at 450 nm.

The total amount of protein was also estimated using the Bradford assay and was found to be very similar to the estimated concentration of protein using the above extinction coefficient, indicating that the protein is fully occupied with FAD. The purity of the sample was estimated from a SDS-PAGE gel stained with Coomassie blue.

2.6. Product detection: HPLC and GC analysis

All separations were performed using pure analytical standards of Ethionamide, Ethionamide-SO, 4-phenyl-2-butanone, phenethyl acetate, 2-octanone, hexyl acetate, 2-decanone, octyl acetate, 2-dodecanone, methyl undecanoate, decyl acetate. Known concentrations of analytical standards were also used to quantify the product formation. HPLC analysis was performed with an Agilent 1200 quaternary pump HPLC System (Agilent Technologies, Italy) with a C18 reverse phase column (LiChroCART 250-4 column packed with Lichrosphere RP C18 5 μM). Previously published methods to separate Ethionamide, Ethionamide-SO, Tozasertib and Tozasertib NO were used [2,9].

The GC analyses were performed with a 7890A GC System (Agilent Technologies, Italy) with a DB-Wax column (Length 30 m; Diameter 0.320 mm; PEG film 0.25 μM). The 4-phenyl-2-butanone and phenethyl acetate were separated following a published protocol [9].

The separation method of 2-octanone and hexyl acetate consisted in the following steps: Oven start at 50 °C; to 80 °C at 10 °C/min; to 230 °C at 25 °C/min; to 250 °C at 20 °C/min; 250 °C hold 5 min; the carrier gas was He (at 3 mL/min). The FID (Flame Ionization Detector) was set at 275 °C. Using this method, the retention times were found to be 5.3 min and 5.1 min for 2-octanone and hexyl acetate, respectively.

The method to separate the 2-decanone and octyl acetate consisted of the following steps: Oven start at 100 °C; to 250 °C at 10 °C/min. The carrier gas was He (at 3 mL/min) and the FID (Flame Ionization Detector) was set to 275 °C. The retention times were 4.5 min and 4.2 min, respectively.

The method to separate the 2-dodecanone, methyl undecanoate and decyl acetate consisted in the following steps: Oven start at 100 °C; to 250 °C at 10 °C/min. The carrier gas was He (at 3 mL/min) and the FID (Flame Ionization Detector) was set at 275 °C. The retention times were 6.5 min, 6.4 min and 6.2 min, respectively.

2.7. Steady state parameters

The steady state kinetic parameters for 4-phenyl-2-butanone, 2-octanone, 2-decanone and 2-dodecanone were determined spectrophotometrically by monitoring the NADPH consumption rates (AU/s) at 340 nm with a series of concentrations of substrates. Samples in a total volume of 0.5 mL contained 0.5 μM enzyme and 150 μM of co-substrate. Reactions were carried out for 5 min at 30 °C in 50 mM potassium phosphate buffer, pH 7.4.

The steady-state kinetic parameters for ethionamide or tozasertib as substrate were obtained using HPLC methodology as described above, with the reactions carried out at 37 °C.

2.8. Mechanistic studies

A Hi-Tech scientific SF-61 (TgK scientific, UK) single mixing stopped-flow system equipped with a diode array detector was used for the mechanistic studies. All experiments were performed in 50 mM potassium phosphate buffer pH 7.4, at 15 °C in a glove box (Belle Technologies, UK) which maintained an O_2 concentration below 10 ppm. Anaerobic reduction of the FAD cofactor of the BVMO enzyme by NADPH/NADH was followed in the stopped-flow apparatus. Each shot mixed 50 μL of purified enzyme (50 μM) with 50 μL of buffer supplemented with NADPH or NADH (100 μM); thus, samples were diluted by half in the mixing cell during the kinetic measurements. Normalized 450 nm absorbance values were fitted with SigmaPlot 9 software to exponential decay equations with 3 parameters ($y = y_0 + ae^{-bx}$) where b represents the measured relaxation rate.

Re-oxidation experiments were performed as follows: first, the BVMO enzyme was fully reduced with NADPH (1 equivalent) or sodium dithionite in anaerobiosis. The completely reduced enzyme in the stopped-flow apparatus was then mixed with an equal volume of oxygenated buffer or with oxygenated buffer containing 1000 μM of the substrate benzylacetone. Each shot was followed for 500 s for the co-substrate reduced enzyme and 9.6 s for the sodium dithionite reduced enzyme. Normalized 450 nm absorbance values were fitted with SigmaPlot 9 software using exponential rise to maximum equations with 3 parameters ($y = y_0 + a(1 - e^{-bx})$) where b is the measured rate.

2.9. Isothermal calorimetry (ITC)

ITC experiments were performed with an ITC-200 calorimeter (Malvern Instruments, Worcestershire, UK). The volume of the calorimetric cell was 0.2 mL, and the titrations were conducted by adding the titrant in steps of 1 μL . Experiments were performed at 25 °C with a 180 s initial delay. All solutions were thoroughly degassed to prevent bubble formation in the cell due to stirring. Freshly prepared Ar-BVMO was dialyzed extensively against degassed buffer containing 50 mM potassium phosphate (pH 7.4 at 4 °C). The protein and NADP concentrations were 8 μM and 800 μM , respectively. Ligand solution was prepared in the flow-through of the dialyzed protein samples. Protein and ligand samples were quickly pre-incubated to the required temperature using a ThermoVac (Malvern Instruments) and loaded in the calorimetric cell and titration syringe, respectively. The titration cell was stirred continuously at 700 rpm. The binding isotherms were best fit to a one-set binding site model by Marquardt nonlinear least-squares analysis to obtain the binding stoichiometry (N), association constant (KA), and thermodynamic parameters of the interaction using ORIGIN software, Version 7 (Malvern Instruments).

2.10. H_2O_2 measurement

The Amplex Red assay (Thermo Fisher Scientific) was used to quantify the H_2O_2 produced. Incubations contained 100 μM NADPH, 1 mM Benzylacetone and 10 nM purified Ar-BVMO. Samples and standards were analyzed in 96 well plates (50 μL /well). A working solution of 100 mM Amplex Red reagent, 0.2 U/mL horseradish peroxidase, 50 mM sodium phosphate pH 7.4 added to each well in a 1:1 volume and incubated 60 min at 37 °C. The absorbance at 340 nm (NADPH consumption) and 572 nm (H_2O_2 formation) was measured for 1 h at 30 s time intervals.

2.11. Site-directed mutagenesis

The primers used for the site-directed mutagenesis were:

Forward-R292G: 5'GCTATAATCCATGGGATCAAGGCCCTTTGTGTAG TGC-3', Reverse-R292G: 5'GCACTACACAAAGGCCCTTGATCCCATGGATTA TAGC-3', Forward-R292A: 5'GCTATAATCCATGGGATCAAGGCCCTTTGTGT

ACTGC-3' and Reverse-R292A: 5'GCACTACACAAAGGGCTTGATCCCAT GGATTATAGC-3'.

PCR reactions were carried out in a final volume of 20 μ L containing: 0.25 μ M of each primer; 0.4 μ L of template (50 ng/ μ L of pT7-BVMO vector), 1 mM MgSO₄, 0.2 mM dNTPs, 2 μ L of 10 \times KOD Buffer (Merck, Germany), 0.02 U of KOD Hot Start DNA polymerase (Merck, Germany). The PCR reactions were performed using a Techne TC-312 thermal cycler (Bibby Scientific Limited, UK) with the following sequence: denaturation at 95 °C for 2 min; 30 cycles at 95 °C for 1 min, 55 °C for 1 min and 70 °C for 2 min and 30 s; this was followed by a final extension at 70 °C for 5 min. PCR products were digested for 2 h at 37 °C with *DpnI* enzyme (Fermentas) to eliminate parental DNA. *E. coli* DH5 α competent cells were subsequently transformed with the *DpnI*-digested PCR product. The transformation reactions were plated onto agar plates supplemented with ampicillin (100 μ g/mL). Plates were incubated at 37 °C for 16 h. The colonies were initially screened for the presence of the BVMO gene and, the R292G and R292A mutations were confirmed by DNA sequencing. The two mutants were expressed and purified with the WT-Ar-BVMO protocols described above.

2.12. Activity assay of the mutants

For all three enzymes (WT Ar-BVMO, R292G, R292A) the reactions were performed with the same concentrations of each substrate in 50 mM potassium phosphate buffer pH 7.4. For ethionamide, the reactions were performed in a final volume of 200 μ L with 0.25 μ M enzyme, 500 μ M NADPH, and followed for 10 min at 37 °C. For 2-octanone, the reactions were performed for 30 min at 37 °C in a final volume of 500 μ L with 0.2 μ M enzyme and 200 μ M NADPH. For 4-phenyl-2-butanone, the reactions were performed for 30 min at 37 °C in a final volume of 500 μ L with 0.1 μ M enzyme and 200 μ M NADPH.

3. Results and discussion

The newly discovered Ar-BVMO was heterologously expressed, purified, and characterized with respect to substrate and cofactor preferences, reaction intermediates and involvement of the active site R292 to the overall catalysis.

3.1. Cloning, expression and purification of recombinant Ar-BVMO

The ORF of the putative protein (1491 bp) was amplified via PCR using primers with the restriction sites of *Bam*HI and *Eco*RI. The amplified construct was cloned into the pT7 expression vector using the same two restriction sites [17,18] and finally sequenced to confirm the

correct, in frame insertion of the gene. *Escherichia coli* BL21 (DE3) was chosen as expression system and was transformed with the pT7-BVMO construct. Preliminary expression was carried out in flasks before the process was scaled-up to a 5 L fermenter. An expression time course was carried out to determine the best time for maximal Ar-BVMO protein expression. A clear overexpressed band at the appropriate molecular weight of 57 kDa was observed on SDS-PAGE gel starting from 2 h post-induction with IPTG (data not shown). However, maximal protein production was found to be at 20 h post-induction.

In order to investigate the cellular localization of the protein, the DAS server (Dense Alignment Surface method) was used to predict the local hydrophobicity of the protein, confirming the absence of any trans-membrane domains (Fig. 1A) [20]. The primary sequence of the BVMO enzyme was deduced in silico from the ORF of the gene using the Translate tool of ExPASy Proteomics Server [21] and consisted of 502 amino acids (including the engineered 6 histidine tag at the C-terminus) with a predicted molecular weight of 57 kDa.

While the *E. coli* BL21 expression system is optimal for a fast and high yield expression of proteins, it can also lead to both misfolded protein in inclusion bodies and enzymes predominantly in the apo-form. To overcome these problems and to increase both the yield and quality of the final recovered protein, the post-induction temperature was lowered to 24 °C. The majority of the recombinant Ar-BVMO protein was found in the cytosolic fraction but the addition of Igepal (a nonionic, non-denaturing detergent) increased the final yield of the purified recombinant holo-enzyme by ~30%. Despite the in silico prediction of being cytosolic, Ar-BVMO probably has some local hydrophobic surface patches that render it membrane-associated, similarly to the EtaA BVMO of *Mycobacterium tuberculosis* [11], since in the absence of the nonionic Igepal from the purification buffers less protein was recovered.

The recombinant Ar-BVMO was purified using two chromatography columns: first, a DEAE column and second, a Ni-affinity resin that tightly retained the protein due to engineered His-tag at the C-terminus. The eluted protein from this latter resin led to nearly 100% pure protein as deduced from a Coomassie blue stained SDS-PAGE gel that revealed a single band at approximately 57 kDa, in agreement with the in silico prediction (Fig. 1B). The final yield of the pure protein was 8 ± 2 mg per liter of culture and was calculated based on the extinction coefficient of the protein at 450 nm ($13,900 \text{ M}^{-1} \text{ cm}^{-1}$) together with the Bradford protein assay.

3.2. Search for Ar-BVMO substrates

Because the sequence of Ar-BVMO is more closely related to that of EtaA than other known BVMO enzymes [9], known substrates of EtaA

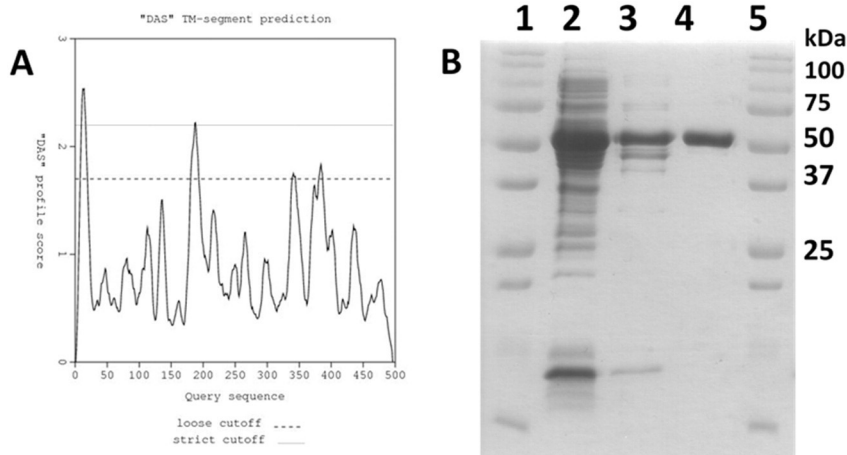


Fig. 1. (A) Hydropathy plot of Ar-BVMO using the DAS-TM program. (B) 10% SDS-PAGE gel of purified Ar-BVMO: Lane 1 and 5 protein markers, Lane 2 crude extract; Lane 3 first purification step (DEAE); Lane 4 second purification step (Ni-affinity).

from *M. tuberculosis* [12] were initially considered. Therefore, the EtaA substrates, 2-octanone, 2-decanone and 2-dodecanone, were selected and following incubation with purified Ar-BVMO they were found to be converted into hexyl acetate, octyl acetate and a mixture of methyl undecanoate ($8 \pm 1\%$) and decyl acetate ($92 \pm 1\%$), respectively. The corresponding GC traces of the controls together with the reaction products are shown in Fig. 2.

The steady-state kinetic parameters for the conversion of 2-octanone and 2-decanone by purified Ar-BVMO were determined spectrophotometrically at 340 nm to monitor the NADPH consumption rates. Apparent Michaelis constants (K_m) values of $351 \pm 60 \mu\text{M}$ and $66 \pm 11 \mu\text{M}$ together with turnover rates (k_{cat}) of 1.3 s^{-1} and 1.6 s^{-1} were calculated for 2-octanone and 2-decanone, respectively. The steady-state kinetics data are summarized in Table 1. Incubations

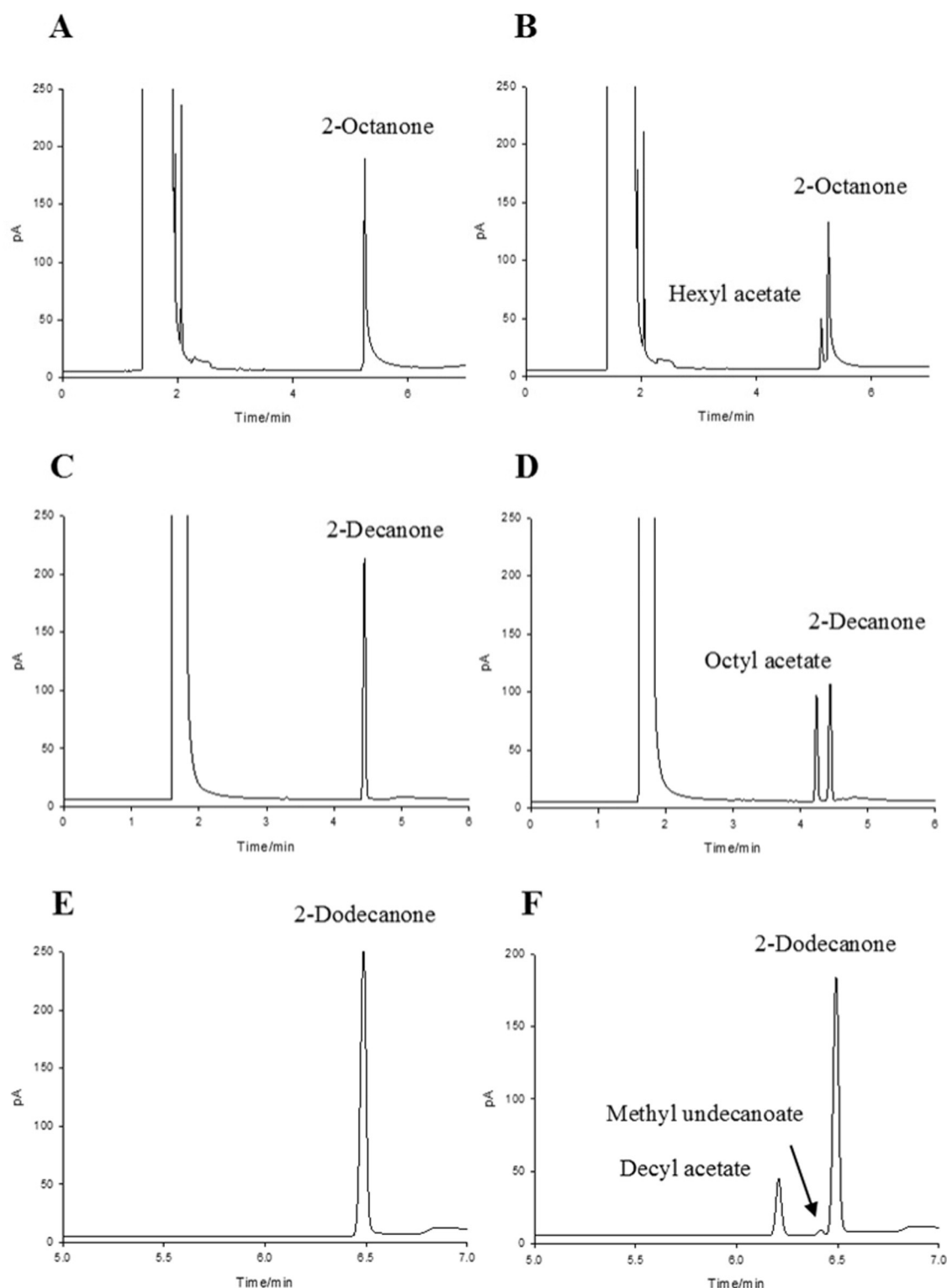


Fig. 2. GC chromatograms of incubations of 2-octanone, 2-decanone and 2-dodecanone in the absence (A, C, E) and presence (B, D, F) of purified Ar-BVMO.

Table 1
Steady-state kinetic parameters of Ar-BVMO determined by rates of NADPH consumption.

Substrate	Reaction	K_m [μM]	k_{cat} [s^{-1}]	k_{cat}/K_m [$10^3 \text{ s}^{-1} \text{ M}^{-1}$]
Tozasertib ^a		54 ± 8	0.11	1.95
Ethionamide ^{a,b}		768 ± 57	0.3	0.4
4-Phenyl-2-Butanone		696 ± 322	0.3	0.4
2-Octanone		351 ± 60	1.3	3.7
2-Decanone		66 ± 11	1.6	24
2-Dodecanone		nd	nd	

^aSubstrates previously identified [2,14];

^b K_m determined by quantifying the product formed using HPLC at different concentrations of substrate.

were performed with concentrations of substrate between 0–3 mM. As can be seen in the Table 1, the best substrate among those tested is 2-decanone with a catalytic efficiency of $2.4 \times 10^4 \text{ M}^{-1} \text{ s}^{-1}$. Steady-state kinetic parameters of Ar-BVMO were also measured in the absence of substrate where it displayed a basal NADPH oxidase activity with a k_{cat} value of 0.09 s^{-1} and a K_m of $14 \mu\text{M}$.

The K_m values measured for all these substrates were in the micromolar range with k_{cat} values comparable to those reported for other previously studied BVMO enzymes [4,22]. As can be seen in the above table, all of the turnover rates (k_{cat}) for the tested substrates are quite similar but the K_m values differ. Similar observations have been made in other BVMOs [4,8], suggesting that the maximal turnover rate does not depend on the reactivity of the flavin intermediate with the substrate but rather the release of NADP^+ in the final step of the catalytic cycle. As a consequence, the release of NADP^+ limits the turnover number. In order to test whether Ar-BVMO turnover is also limited by the NADP^+ release, the affinity of the enzyme for the oxidized form of NADP^+ was measured using ITC. As expected, Ar-BVMO showed a high affinity for the oxidized cofactor (Fig. 3) with a calculated K_d value of $8.3 \mu\text{M}$.

3.3. Ar-BVMO reduction with NADH and NADPH

For the Group B flavoprotein monooxygenases [23], including BVMO enzymes, the reduction of the FAD by the co-substrate occurs in a substrate independent manner [24,25]. It is also known that class I BVMOs are specific for NADPH and not NADH as the electron donor for catalysis [5]. Stopped-flow experiments of the reductive half-reactions of Ar-BVMO were carried out using each of the two co-substrates. Although both NADPH and NADH reduced the enzyme, NADPH was somewhat faster in reducing the FAD group. Reactions with both co-enzymes are biphasic (Fig. 4) and were fitted to a double exponential corresponding to a fast and a slow rate. The calculated fast reduction rates were $12.8 \pm 2.0 \text{ s}^{-1}$ and $21.2 \pm 4.0 \text{ s}^{-1}$ with calculated slow rates of 0.15 ± 0.03 and 0.16 ± 0.01 for NADH and NADPH, respectively. This observed biphasic nature of the reduction rates is most probably due to some residual oxygen in the system.

This difference is likely due to a more favored binding between NADPH and BVMO. To confirm if the reduction of Ar-BVMO by each co-enzyme subsequently led to oxygenation, reactions were performed with each of the co-enzymes using 4-phenyl-2-butanone as substrate. The ester product, phenethyl acetate, analyzed by GC, was only

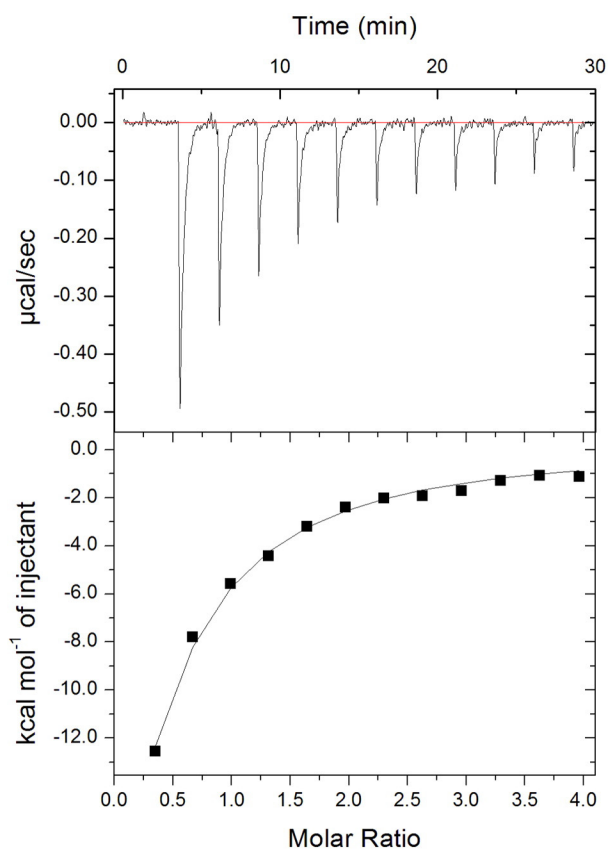


Fig. 3. Isothermal calorimetric titration of NADP ($800 \mu\text{M}$) with purified Ar-BVMO ($12.5 \mu\text{M}$) in 50 mM potassium phosphate buffer pH 8 at $25 \text{ }^\circ\text{C}$. Heat variation generated by each injection of titrant at each time interval (top panel) and the integration of each peak and the amount of heat produced (lower panel).

observed in good yields with NADPH as reductant, suggesting that in contrast to NADP^+ , NAD^+ does not bind tightly to the reduced enzyme.

3.4. Measurement of the C4a-(hydro)peroxyflavin intermediate

The oxidative half-reaction of Ar-BVMO was studied by stopped-flow techniques in an anaerobic glove box. The enzyme was reduced by 1 equivalent of NADPH in one syringe and then mixed with air-saturated buffer (50 mM potassium phosphate buffer, pH 7.4) from the second syringe. Fig. 5A shows that the formation of the the C4a-(hydro)peroxyflavin intermediate at 375 nm requires $\sim 40 \text{ s}$ to be complete. This contrasts with CHMO, which forms the C4a-intermediate within the dead time of the stopped-flow instrument, 1–2 ms [8]. The intermediate then decays as shown by the increase in absorbance at 450 nm (Fig. 5A) in a time scale longer than 300 s .

If the same re-oxidation experiments are carried out in the presence of a substrate (benzylacetone), the C4a-(hydro)peroxyflavin intermediate is formed within 0.5 s (Fig. 5B), and the re-oxidation is much faster, with conversion to the fully oxidized form being complete within 7 s . The presence of the substrate accelerates the decay of the C4a-(hydro)peroxyflavin to the oxidized FAD by ~ 30 -fold. These results demonstrate that the reoxidation of the enzyme in the absence of an appropriate substrate is slow, and occurs in a time scale of $>2 \text{ min}$ with an apparent rate constant of $0.0129 \pm 0.0001 \text{ s}^{-1}$ (Fig. 5C) indicating that the decay of the C4a-(hydro)peroxyflavin is comparable to recent data reported for another BVMO enzyme, BVMOAf1 from *Aspergillus fumigatus* Af293 [26]. Under these conditions, the addition of a saturating concentration of the substrate ($1000 \mu\text{M}$ benzylacetone) to the reduced enzyme increased the re-oxidation rate up to thirty-fold with the estimated rate constant of $0.40 \pm 0.02 \text{ s}^{-1}$. Therefore, in the

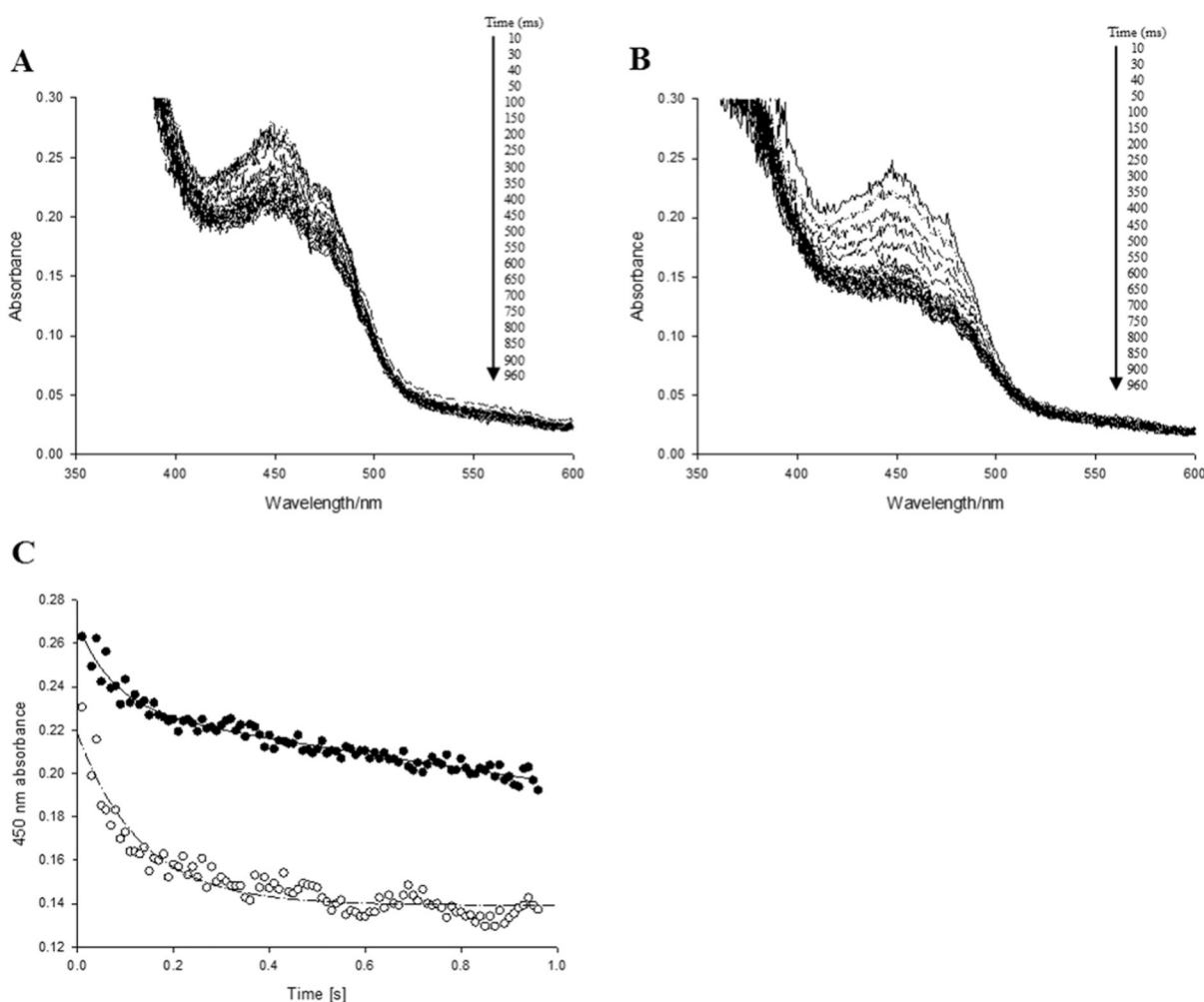


Fig. 4. Ar-BVMO absorbance spectra collected during anaerobic reduction with 2 equivalents of either (A) NADH or (B) NADPH. The experiments were performed in 50 mM potassium phosphate buffer pH 7.4 at 8 °C over 0.96 s at 10 ms intervals. (C) Kinetic analysis of the reduction of the flavin cofactor. Exponential decay fitting of the NADH (closed circles) and NADPH mediated reduction (open circles) fitted to a double exponential: fast reduction rates were $21.2 \pm 4.0 \text{ s}^{-1}$ and $12.8 \pm 2.0 \text{ s}^{-1}$ with calculated slow rates of 0.16 ± 0.01 and 0.15 ± 0.03 for NADPH and NADH, respectively.

presence of the substrate, the absorbance at 450 nm increases very rapidly indicating that both formation and decay of the intermediate are accelerated by the addition of a substrate (Fig. 5C). This finding is in line with other Group B flavin monooxygenases that also show a faster rate of flavin oxidation in the presence of a suitable substrate [27,28].

Previous structural as well as mutagenesis studies have concluded that the C4a-(hydro)peroxyflavin intermediate is stabilized by NADP^+ which remains bound until the last step of the catalytic cycle [8,29–32]. However, if this intermediate is not stabilized or the NADP^+ binding is compromised, the uncoupling of the enzyme results in hydrogen peroxide release. In order to estimate the amount of any H_2O_2 produced by Ar-BVMO during the catalytic cycle the AMPLEX RED assay was performed in the presence of a saturating concentration of benzylacetone (Fig. S1). The results show that the uncoupling of Ar-BVMO, evaluated as the ratio between H_2O_2 formed and NADPH consumed, is about 7–10%, and that the reaction leads to the formation of 3.16 nmol of H_2O_2 /min/nmol Ar-BVMO. Rauckman et al. [33] found that purified pig liver FMO (FMO1) produced superoxide anion radical at the rate of about 4% of the total NADPH oxidized. Tynes et al. [34] found hydrogen peroxide produced by the purified rabbit lung FMO (FMO2) at up to 41% of the total NADPH oxidized. More recently Siddens et al. [35] published data on three human FMOs, where the percentage of molecular oxygen consumed that appeared as H_2O_2 varied between 30 and 50% at a rate of 0.5–2.5 nmol/min/nmol FMO. However, all these uncoupling data are

for mammalian FMO enzymes and to our knowledge no such data has been reported for the bacterial BVMO enzymes.

Finally, the oxidative half-reaction of Ar-BVMO was also monitored in the absence of pyridine nucleotide by using sodium dithionite as the reductant (Fig. 6A). In this case the re-oxidation is complete within 9.6 s, much faster than that observed with NADPH as the electron donor. Moreover, no C4a-flavin peroxide is observed, and the re-oxidation rate is not dependent on the presence of the substrate; re-oxidation rates in the absence/presence of substrate were: $0.39 \pm 0.02 \text{ s}^{-1}$ versus $0.43 \pm 0.02 \text{ s}^{-1}$ (Fig. 6B). As mentioned earlier, the latter nearly identical rates were expected and in line with other BVMO and FMO enzymes where in normal catalysis the NADP^+ remains bound and stabilizes the C4a-intermediate. Therefore, NADPH plays a dual role both as a reductant and in its oxidized form, a promoter of oxygenation, whereas dithionite is solely a flavin reductant.

3.5. Identification of the catalytically determinant R292

In the absence of a crystal structure and in order to investigate the putative active site of Ar-BVMO, a multi-alignment was performed with amino acid sequences of different BVMOs including HAPMO (*Pseudomonas fluorescens*), PAMO (*Thermobifida fusca*), CHMO (*Rhodococcus* sp.), Alma (*Acinetobacter* sp. DSM 17874), EtaA (*M. tuberculosis* H37RV) and Ar-BVMO (*A. radioresistens* S13) as

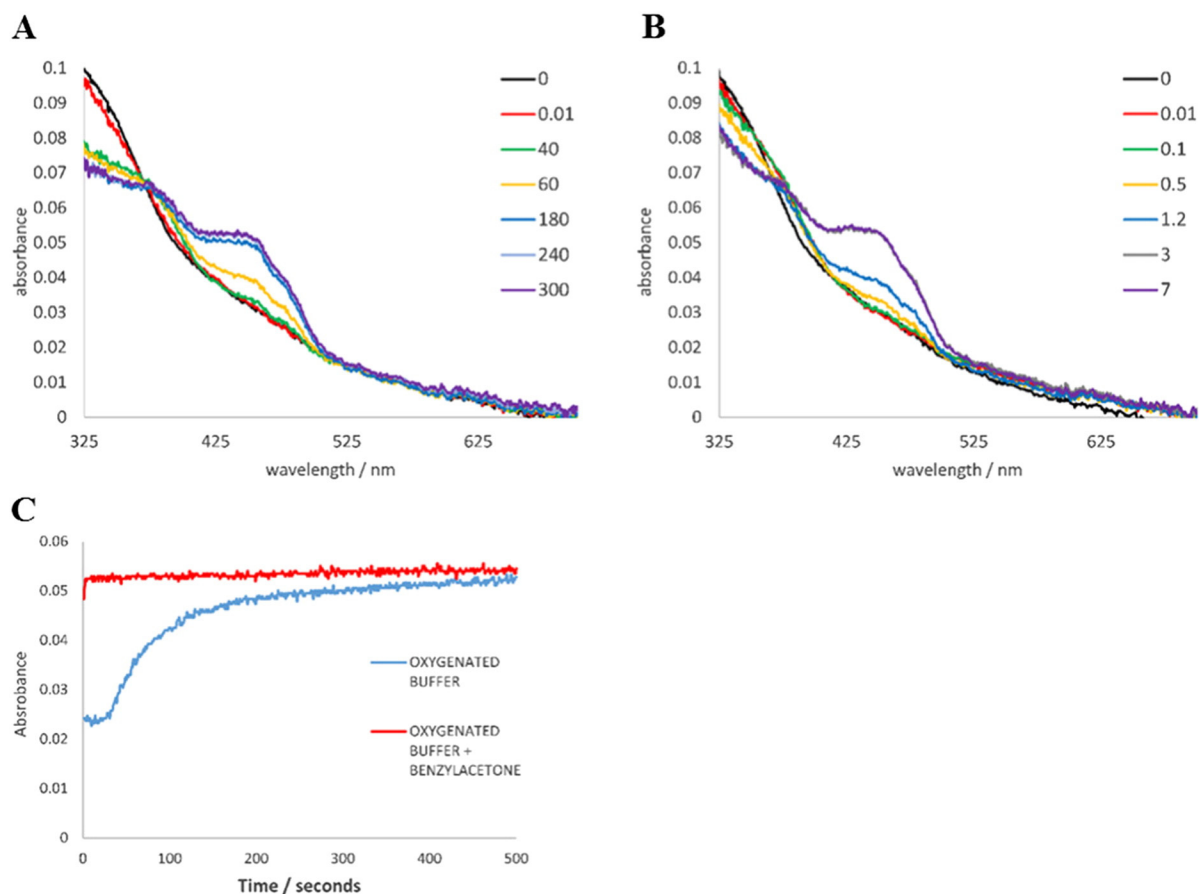


Fig. 5. (A) Formation and decay of the C4a-(hydro)peroxyflavin within 300 s after mixing the NADPH reduced enzyme with air-saturated buffer (without substrate); (B) Formation and decay of the C4a-(hydro)peroxyflavin within 7 s after mixing the NADPH reduced enzyme with air-saturated buffer (with 1000 μM benzylacetone). (C) Comparison of the decay of the C4a-(hydro)peroxyflavin in the presence (red line) and absence of benzylacetone substrate (blue line) followed at 450 nm. The experiment was performed in 50 mM potassium phosphate buffer pH 7.4 at 15 $^{\circ}\text{C}$.

shown in Fig. 7. The conserved Baeyer-Villiger sequence motif FXGXXXHXXW(P/D) [36] is highlighted by the purple box together with the known crucial catalytic conserved arginine residue (red box). This arginine corresponds to R440 in HAPMO, R337 in PAMO and R329 in CHMO. The marked sequence similarity between Ar-

BVMO, Alma and EtaA is once again illustrated, as the conserved arginine is also within a conserved amino acid patch of around 5–10 amino acids (both upstream and downstream). The conserved aspartyl residue, involved in proper positioning of NADPH in the active site of these enzymes [29], is also highlighted in Fig. 7 (D66 in

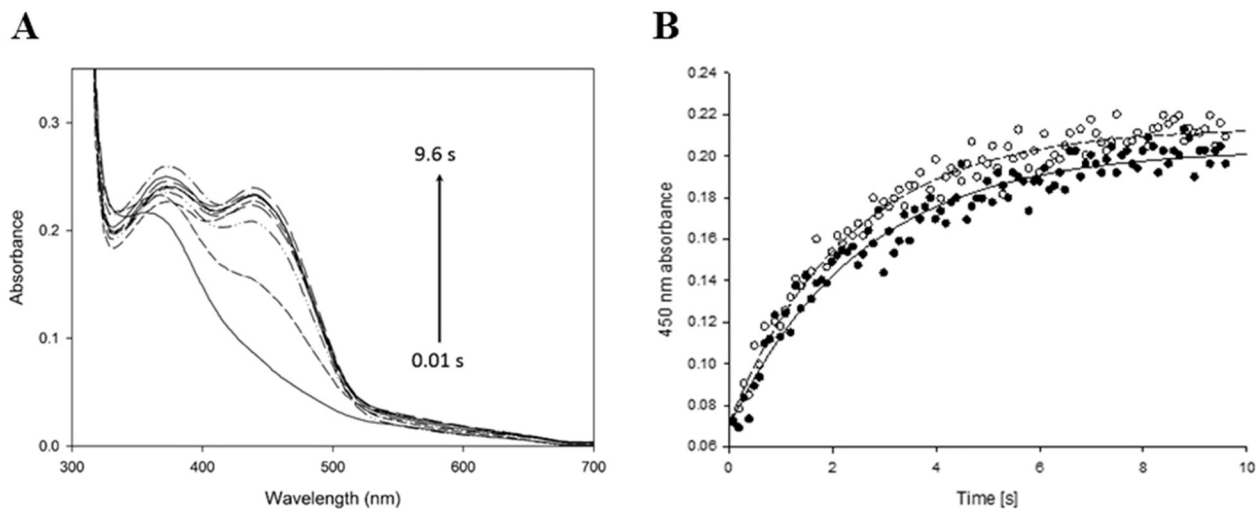


Fig. 6. A) Spectra of the re-oxidation of Ar-BVMO after complete reduction with sodium dithionite and mixing the reduced enzyme with air-saturated buffer. The experiment was performed in 50 mM potassium phosphate buffer pH 7.4 at 8 $^{\circ}\text{C}$ in a 9.6 s time scale. B) Kinetic analysis of the re-oxidation of the flavin cofactor. Exponential rise to maximum fitting of the re-oxidation with oxygenated buffer only (filled circles) and oxygenated buffer with substrate (empty circles). The observed re-oxidation rate constants were $0.39 \pm 0.02 \text{ s}^{-1}$ and $0.43 \pm 0.02 \text{ s}^{-1}$, respectively.

PAMO, D192 in HAPMO, D58 in CHMO and D56 in Alma, EtaA and Ar-BVMO).

The important role played by the conserved arginine in different BVMO enzymes has been previously demonstrated by site-directed mutagenesis. For example, replacing R440 of HAPMO from *Pseudomonas fluorescens* by an alanine resulted in an inactive enzyme [37] while R337 of PAMO from *Thermobifida fusca* replaced by either alanine or lysine still formed the C4a-peroxyflavin intermediate but the enzyme was unable to perform either the Baeyer-Villiger reaction on phenylacetone or the S-oxidation on benzyl methyl sulfide [38]. More recently, a high-resolution crystal structure of PAMO from *T. fusca* [29] explained how the arginine 337 of this enzyme contributes to ketone activation via hydrogen bonding to the carbonyl oxygen of the substrate, thus increasing the electrophilicity of the carbonyl carbon to enhance the nucleophilic attack by the C4a-peroxyflavin intermediate. Furthermore, the same researchers also suggested that this positively charged amino acid together with the NADP ribose moiety, compensates for the negative charge of the Criegee intermediate, hence stabilizing it [29].

In order to understand whether this conserved arginine (R292) also plays an important role in Ar-BVMO, two mutants were designed and generated by site-directed mutagenesis: R292G and R292A. These mutants were expressed and subsequently purified with the same protocol as the WT Ar-BVMO, although with a lower

yield of approximately 4 mg per liter of culture. These two mutants exhibited similar absorbance spectra to that of wild-type Ar-BVMO and were able to oxidize NADPH. The thermal stability of the mutants was also evaluated and compared to the wild type. The observed melting temperatures for R292G and R292A were calculated to be 48.9 ± 0.2 °C and 49.1 ± 0.2 °C, respectively. These values are in good agreement with the measured T_m value of 48.6 ± 0.2 °C for recombinant wild type Ar-BVMO, indicating that the mutants are correctly folded and equally stable.

The Baeyer-Villiger activities of the two mutants, R292G and R292A, were compared to that of the wild type Ar-BVMO enzyme using the two previously identified ketone substrates (4-phenyl-2-Butanone and 2-octanone) and measuring the products formed by GC. The results obtained are shown in Table 2 where drastically reduced Baeyer-Villiger activities of both mutants towards the ketone substrates is demonstrated. In the case of R292A, no product was detected with either 4-phenyl-2-butanone or 2-octanone, whereas the R292G enzyme showed a small residual activity of 1.5% and 4.5% with the same two ketones, respectively. As mentioned earlier, the arginine to alanine mutations in HAPMO and PAMO also resulted in inactive enzymes with no Baeyer-Villiger activity [37,38]. The observed lack of Baeyer-Villiger activity of the two mutants towards the tested ketones confirms the importance of this arginine residue for catalysis [29].

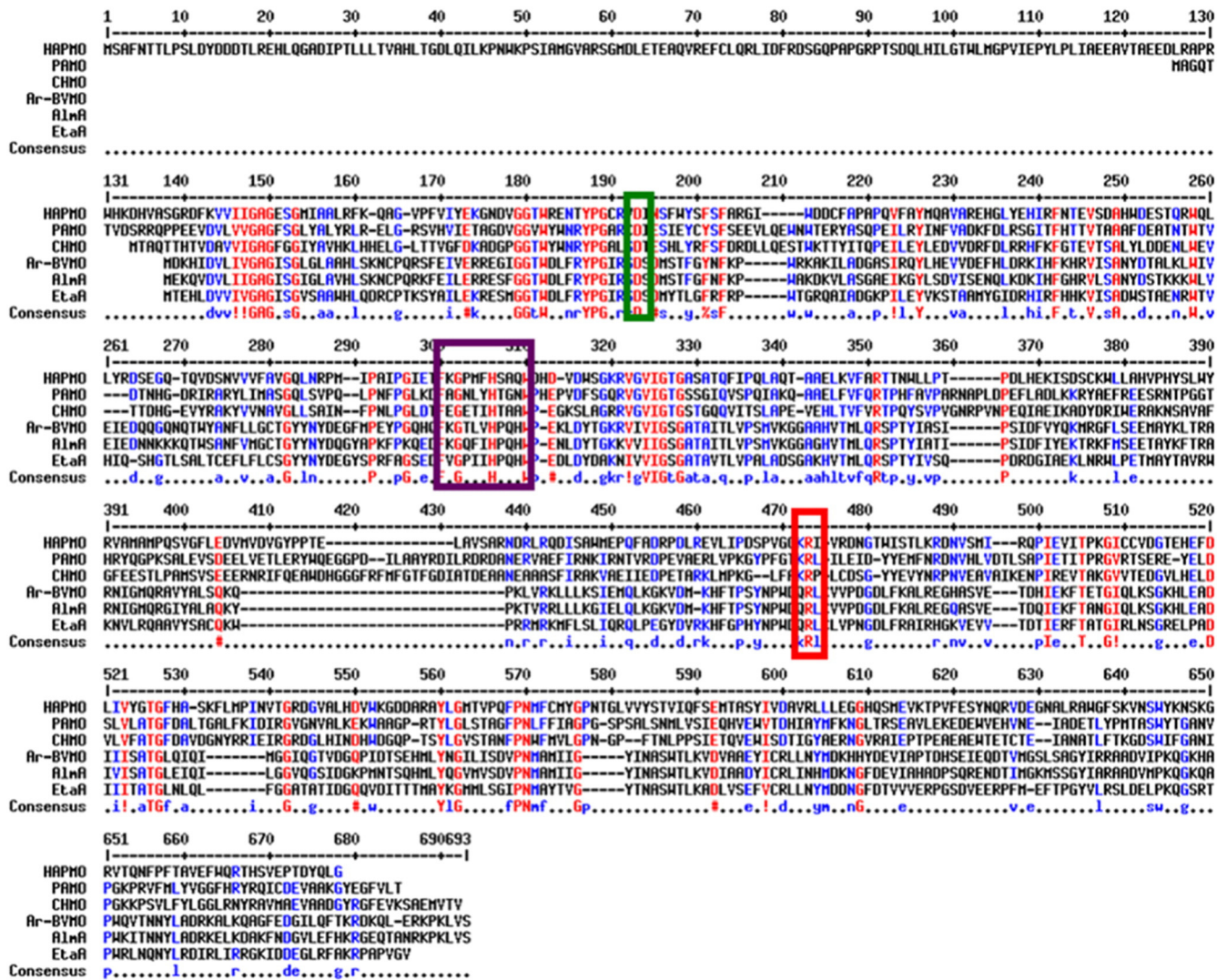


Fig. 7. Multi-alignment of the primary sequences of HAPMO (*P. fluorescens*); PAMO (*T. fusca*); CHMO (*Rhodococcus* sp.); Ar-BVMO (*A. radioresistens* S13); Alma (*Acinetobacter* sp. DSM 17874) and EtaA (*M. tuberculosis* H37RV). The BVMO motif, the conserved arginine and aspartic acid residues are indicated by purple, red and green boxes, respectively. (For interpretation of the references to colour in this figure legend, the reader is referred to the web version of this article.)

In addition, the S-oxygenation and N-oxygenation activity of the mutant enzymes was also compared to that of the purified wild type Ar-BVMO using ethionamide and tozasertib as substrates, quantifying the S-oxide or N-oxide product by HPLC analysis. Both substrates are also known to be metabolized by the human flavin-containing monooxygenase 3 with the formation of the corresponding S- or N-oxides [13–15]. R292A and R292G mutants showed a residual activity of 83.9% and 43.3% respectively when compared to the wild type Ar-BVMO for ethionamide and 60% and 5.3% residual activity for Tozasertib, as shown in Table 2. The fact that replacement of the conserved Arg residue with Ala or Gly exerts an effect on the S- or N-oxygenation reaction could mean that this residue is involved in more than just stabilization of the Criegee intermediate. In this specific case, the size of the amino acid residue seems to have a role in the S- or N-oxygenation activity since the bulkier Ala residue has nearly double the activity of the smaller Gly residue (83.9% versus 43.3% residual activity) suggesting a possible role of Ala in helping the stabilization of the intermediate by excluding water, which could otherwise break down the C4a-intermediate. The effect of the positive charge of the Arg residue is less important for the S- or N-oxygenation reaction, with the activity of the R292A mutant decreased by 16% and 40% for N- and S-oxidation, respectively.

In summary, the data presented here confirm that the conserved arginine, R292, not only plays an important role in the activity of Ar-BVMO but is also crucial for its Baeyer–Villiger reactions. Moreover, the ability of the R292 mutants to catalyze S/N-oxidations is almost certainly associated with the nucleophilic nature of ketone oxygenations, versus the electrophilic nature of heteroatom oxidations by these enzymes.

4. Conclusions

Baeyer–Villiger monooxygenases are FAD-dependent enzymes with broad substrate spectra, and in many cases they exhibit high stereospecificity. Similar to other members of the BVMO group of enzymes, Ar-BVMO shows a tightly but not covalently bound FAD cofactor that can be reduced anaerobically with NADPH. With NADP⁺ product remaining bound, the resulting FADH can react with O₂ to form a flavin C4a-peroxide. This “loaded gun” intermediate of the enzyme can bind any of a variety of substrates, and the flavin C4a-peroxide can effect Baeyer–Villiger reactions with carbonyl substrates or oxidations or oxygenations of thiols, thioethers, or amines. Ar-BVMO also seems to have broad substrate tolerance, which is consistent with the kinetic data presented in this work. The enzyme C4a-(hydro)peroxyflavin intermediate is relatively stable and does not convert rapidly to oxidized flavin rapidly unless a suitable substrate is present. The initial reduction step by NADPH is independent of the substrate and not strictly controlled, presumably because it would be difficult to effect substrate control with the broad substrate acceptance of this enzyme.

The role of the active site Arginine 292 residue of Ar-BVMO in catalysis was investigated by engineering two mutants, R292A and R292G. The R292A variant had no measureable activity and the R292G variant had very little activity in Baeyer–Villiger catalysis. However, the monooxygenation activity with the sulfur-containing substrate ethionamide by the R292A variant was only slightly less than that of wild type Ar-BVMO. An aurora kinase inhibitor, Tozasertib, was also tested

to assess the N-oxidation activity of the mutants. The R292A mutant retained >60% of the activity of the wild type enzyme. The data clearly show that the R292A mutant is not able to perform BV catalysis, but can selectively perform S- or N-oxidations similar to human flavin-containing monooxygenases.

Finally, since Ar-BVMO can be expressed in *E. coli* without inhibiting the host bacterial growth, scaling up the expression of its mutants in fermenters can lead to high yields of these biocatalysts, which can be used for large-scale production of oxidized human FMO metabolites.

Supplementary data to this article can be found online at <http://dx.doi.org/10.1016/j.bbapap.2016.06.010>.

Transparency document

The Transparency document associated with this article can be found, in online version.

References

- G. de Gonzalo, M.D. Mihovilovic, M.W. Fraaije, Recent developments in the application of Baeyer–Villiger monooxygenases as biocatalysts, *ChemBiochem* 11 (2010) 2208–2231.
- D. Minerdi, I. Zgrablic, S. Castrignanò, G. Catucci, C. Medana, M.E. Terlizzi, G. Gribaudo, G. Gilardi, S.J. Sadeghi, *Escherichia coli* overexpressing a Baeyer–Villiger monooxygenase from *Acinetobacter radioresistens* become resistant to imipenem, *Antimicrob. Agents Chemother.* 60 (2016) 64–74.
- W.G. Lai, N. Farah, G.A. Moniz, Y.N. Wong, A Baeyer–Villiger oxidation specifically catalyzed by human flavin-containing monooxygenase 5, *Drug Metab. Dispos.* 39 (2011) 61–70.
- N.M. Kamerbeek, D.B. Janssen, W.J.H. van Berkel, M.W. Fraaije, Baeyer–Villiger monooxygenases, an emerging family of flavin-dependent biocatalysts, *Adv. Synth. Catal.* 345 (2003) 667–678.
- H. Leisch, K. Morley, P.C.K. Lau, Baeyer–Villiger monooxygenases: more than just green chemistry, *Chem. Rev.* 111 (2011) 4165–4222.
- M.D. Mihovilovic, B. Mueller, P. Stanetty, Monooxygenase-mediated Baeyer–Villiger oxidations, *ChemInform* 34 (2002) 3711–3730.
- C.C. Ryerson, D.P. Ballou, C.T. Walsh, Mechanistic studies on cyclohexanone oxygenase, *Biochemistry* 21 (11) (1982) 2644–2655.
- D. Sheng, D.P. Ballou, V. Massey, Mechanistic studies of cyclohexanone monooxygenases: chemical properties of intermediates involved in catalysis, *Biochemistry* 40 (2001) 11156–11167.
- D. Minerdi, S.J. Sadeghi, G. Di Nardo, F. Rua, S. Castrignanò, P. Allegra, G. Gilardi, CYP116B5: a new class VII catalytically self-sufficient cytochrome P450 from *Acinetobacter radioresistens* that enables growth on alkanes, *Mol. Microbiol.* 95 (2014) 539–554.
- A.E. DeBarber, K. Mdluli, M. Bosman, L.-G. Bekker, C.E. Barry, Ethionamide activation and sensitivity in multidrug-resistant *Mycobacterium tuberculosis*, *Proc. Natl. Acad. Sci.* 97 (2000) 9677–9682.
- T.A. Vannelli, A. Dykman, P.R. Ortiz de Montellano, The antituberculosis drug ethionamide is activated by a flavoprotein monooxygenase, *J. Biol. Chem.* 277 (2002) 12824–12829.
- M.W. Fraaije, N.M. Kamerbeek, A.J. Heidekamp, R. Fortin, D.B. Janssen, The prodrug activator EtaA from *Mycobacterium tuberculosis* is a Baeyer–Villiger monooxygenase, *J. Biol. Chem.* 279 (2004) 3354–3360.
- D. Minerdi, I. Zgrablic, S.J. Sadeghi, G. Gilardi, Identification of a novel Baeyer–Villiger monooxygenase from *Acinetobacter radioresistens*: close relationship to the *Mycobacterium tuberculosis* prodrug activator EtaA, *Microb. Biotechnol.* 5 (2012) 700–716.
- G. Catucci, G. Gilardi, L. Jeuken, S.J. Sadeghi, In vitro drug metabolism by C-terminally truncated human flavin-containing monooxygenase 3, *Biochem. Pharmacol.* 83 (2012) 551–558.
- G. Catucci, A. Occhipinti, M. Maffei, G. Gilardi, S.J. Sadeghi, Effect of human flavin-containing monooxygenase 3 polymorphism on the metabolism of aurora kinase inhibitors, *Int. J. Mol. Sci.* 14 (2013) 2707–2716.
- Y. Chen, N.A. Patel, A. Crombie, J.H. Scrivens, J.C. Murrell, Bacterial flavin-containing monooxygenase is trimethylamine monooxygenase, *Proc. Natl. Acad. Sci. U. S. A.* 108 (2011) 17791–17796.
- H. Li, K. Darwish, T.L. Poulos, Characterization of recombinant bacillus megaterium cytochrome P-450sM-a3nd its two functional domain, *J. Biol. Chem.* 266 (1991) 11909–11914.
- F. Valetti, S.J. Sadeghi, Y.T. Meharena, S.R. Leliveld, G. Gilardi, Engineering multidomain redox proteins containing flavodoxin as bio-transformer: preparatory studies by rational design, *Biosens. Bioelectron.* 13 (1998) 675–685.
- L.G. Whitby, A new method for preparing flavin-adenine dinucleotide, *Biochem. J.* 54 (1953) 437–442.
- M. Cserzo, E. Wallin, I. Simon, G. von Heijne, A. Elofsson, Prediction of transmembrane alpha helices in prokaryotic membrane proteins: the dense alignment surface method, *Protein Eng.* 10 (1997) 673–676.
- P. Artimo, M. Jonnalagedda, K. Arnold, D. Baratin, G. Csardi, E. de Castro, S. Duvaud, V. Flegel, A. Fortier, E. Gasteiger, A. Grosdidier, C. Hernandez, V. Ioannidis, D. Kuznetsov, R. Liechti, S. Moretti, K. Mostaguir, N. Redaschi, G. Rossier, I. Xenarios,

Table 2

Activity of the two Ar-BVMO mutants with different substrates compared to the wild type enzyme.

BVMO	Substrate			
	2-octanone	4-phenyl-2-butanone	Ethionamide	Tozasertib
WT	100%	100%	100%	100%
R292A	nd ^a	nd ^a	83.9%	60%
R292G	4.6%	1.5%	43.3%	5.3%

^a Not detectable.

- H. Stockinger, ExPASy: SIB bioinformatics resource portal, *Nucleic Acids Res.* 40 (W1) (2012) W597–W603.
- [22] W.A. Duetz, J.B. van Beilen, B. Witholt, Using proteins in their natural environment: potential and limitations of microbial whole-cell hydroxylations in applied biocatalysis, *Curr. Opin. Biotechnol.* 12 (2001) 419–425.
- [23] W.J.H. van Berkel, N.M. Kamerbeek, M.W. Fraaije, Flavoprotein monooxygenases, a diverse class of oxidative biocatalysts, *J. Biotechnol.* 124 (2006) 670–689.
- [24] N.B. Beaty, D.P. Ballou, The reductive half-reaction of liver microsomal FAD-containing monooxygenase, *J. Biol. Chem.* 256 (1981) 4611–4618.
- [25] N.B. Beaty, D.P. Ballou, The oxidative half-reaction of liver microsomal FAD-containing monooxygenase, *J. Biol. Chem.* 256 (1981) 4619–4625.
- [26] M.L. Mascotti, M. Kurina-Sanz, M. Juri-Ayub, M.W. Fraaije, Insights in the kinetic mechanism of the eukaryotic Baeyer–Villiger monooxygenase BVMOA1 from *Aspergillus fumigatus* Af293, *Biochimie* 104 (2014) 270–276.
- [27] X. Dai, K. Mashiguchi, Q. Chen, H. Kasahara, Y. Kamiya, S. Ojha, J. DuBois, D.P. Ballou, Y. Zhao, The biochemical mechanism of auxin biosynthesis by an *Arabidopsis* YUCCA flavin-containing monooxygenase, *J. Biol. Chem.* 288 (2013) 1448–1457.
- [28] J.A. Mayfield, R.E. Frederick, B.R. Streit, T.A. Wenczewicz, D.P. Ballou, J.L. DuBois, Comprehensive spectroscopic, steady state, and transient kinetic studies of a representative siderophore-associated flavin monooxygenase, *J. Biol. Chem.* 285 (2010) 30375–30388.
- [29] R. Orru, H.M. Dudek, C. Martinoli, D.E. Torres Pazmiño, A. Royant, M. Weik, M.W. Fraaije, A. Mattevi, Snapshots of enzymatic Baeyer–Villiger catalysis: oxygen activation and intermediate stabilization, *J. Biol. Chem.* 286 (2011) 29284–29291.
- [30] I. Ahmad Mirza, J.B. Yachnin, S. Wang, S. Grosse, H. Bergeron, A. Imura, H. Iwaki, Y. Hasegawa, P.C.K. Lau, A.M. Berghuis, Crystal structures of cyclohexanone monooxygenase reveal complex domain movements and a sliding cofactor, *J. Am. Chem. Soc.* 131 (2009) 8848–8854.
- [31] B.J. Yachin, T. Sprules, M.B. McEvoy, P.C.K. Lau, A.M. Berghuis, The substrate-bound crystal structure of a Baeyer–Villiger monooxygenase exhibits a criegee-like conformation, *J. Am. Chem. Soc.* 134 (2012) 7788–7795.
- [32] E. Malito, A. Alfieri, M. Fraaije, A. Mattevi, Crystal structure of a Baeyer–Villiger monooxygenases, *Proc. Natl. Acad. Sci.* 101 (2004) 13157–13162.
- [33] E.J. Rauckman, M.G. Rosen, B.B. Kitchell, Superoxide radical as an intermediate in the oxidation of hydroxylamines by mixed function amine oxidase, *Mol. Pharmacol.* 15 (1979) 131–137.
- [34] R.E. Tynes, P.J. Sabourin, E. Hodgson, R.M. Philpot, Formation of hydrogen peroxide and N-hydroxylated amines catalyzed by pulmonary flavin-containing monooxygenases in the presence of primary alkylamines, *Arch. Biochem. Biophys.* 251 (1986) 654–664.
- [35] L.K. Siddens, S.K. Krueger, M.C. Henderson, D.E. Williams, Mammalian flavin-containing monooxygenase (FMO) as a source of hydrogen peroxide, *Biochem. Pharmacol.* 89 (2014) 141–147.
- [36] M.W. Fraaije, N.M. Kamerbeek, W.J.H. van Berkel, D.B. Janssen, Identification of a Baeyer–Villiger monooxygenase sequence motif, *FEBS Lett.* 518 (2002) 43–47.
- [37] R.H.H. van den Heuvel, N. Tahallah, N.M. Kamerbeek, M.W. Fraaije, J. Willem, H. van Berkel, D.B. Janssen, A.J.R. Heck, Coenzyme binding during catalysis is beneficial for the stability of 4-hydroxyacetophenone monooxygenase, *J. Biol. Chem.* 280 (2005) 32115–32121.
- [38] D.E. Torres Pazmiño, B.-J. Baas, D.B. Janssen, M.W. Fraaije, Kinetic mechanism of phenylacetone monooxygenase from *Thermobifida fusca*, *Biochemistry* 47 (2008) 4082–4093.